Long period comet encounters with the planets: an analytical approach

G. B. Valsecchi
IAPS-INAF, Roma, Italy
IFAC-CNR, Sesto Fiorentino, Italy

The engine of cometary orbital evolution

- The orbital evolution of comets in the planetary region is mostly due to close encounters with the giant planets.
- An important parameter is the planetocentric velocity:
    - fast encounters – with hyperbolic planetocentric orbits – are effective only if deep;
    - slow encounters – with temporary satellite captures – can greatly modify cometary orbits even if rather shallow.
- The outcomes can be extremely sensitive to initial conditions.
- Long-period comets practically never undergo “really slow” encounters.

Why an analytical theory

The orbits of long period comets are not restricted to low inclinations; among the consequences of this, we have:

- wide range of encounter velocities;
- extended time spans without encounters, due to large MOIDs with respect to the giant planets.

An analytical theory of close encounters can help to:

- identify regions of interest in the space of initial conditions, minimizing the need to run long numerical integrations in which "nothing happens";
- get a global understanding of the possible outcomes of close encounters.

Extended Öpik's theory of close encounters

Model: restricted, circular, 3-dimensional 3-body problem; far from the planet, the small body moves on an unperturbed heliocentric keplerian orbit.

The encounter with the planet: modelled as an instantaneous transition from the incoming asymptote of the planetocentric hyperbola to the outgoing one, taking place when the small body crosses the *b*-plane (O76, CVG90).

Our contribution: added equations to take into account the finite nodal distance and the time of passage at the relevant node (VMGC03, V06, VAR15).

Limitation: this model does not take into account the secular variation of the nodal distance, that has to be given as an additional input.

Encounter algorithm

pre-encounter		post-encounter
$a, e, i, \Omega, \omega, f_b$		$a', e', i', \Omega', \omega', f_b'$
$\downarrow$		$\uparrow$
X, Y, Z, U_x, U_y, U_z		$X', Y', Z', U_x', U_y', U_z'$
$\downarrow$		$\uparrow$
$U, \theta, \phi, \xi, \zeta, t_b$	$\Longrightarrow$	$U, \theta', \phi', \xi', \zeta', t_b$

The algorithmic path describing an encounter:

- we go from orbital elements to planetocentric coordinates and velocities describing a rectilinear motion;
- we pass from coordinates and velocities to Öpik variables;
- we apply the velocity vector rotation due to the encounter;
- we then retrace the same steps in the opposite order, back to orbital elements.

Geometric setup

The reference frame (X, Y, Z) is planetocentric, with the Y-axis in the direction of motion of the planet, and the Sun on the negative X-axis.

The direction of the incoming asymptote is defined by two angles, θ and ϕ, so that the planetocentric unperturbed velocity $\vec{U}$ has components:

$$U_x = U \sin\theta \sin\phi; \quad U_y = U \cos\theta; \quad U_z = U \sin\theta \cos\phi.$$

As a consequence of an encounter the direction of $\vec{U}$ changes but its modulus U does not.

$$\begin{aligned} U &= U(a, e, i) \\ \theta &= \theta(a, e, i) = \theta(a, U) \\ \phi &= \phi(a, e, i) \end{aligned}$$

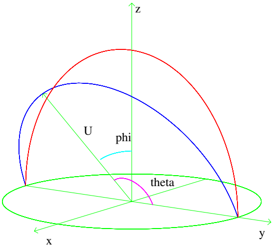

The b-plane

- The b-plane of an encounter is the plane containing the planet and perpendicular to the planetocentric unperturbed velocity $\vec{U}$.
- The vector from the planet to the point in which $\vec{U}$ crosses the plane is $\vec{b}$, and the coordinates of the crossing point are ξ, ζ.
- The coordinate $\xi = \xi(a, e, i, \omega, f)$ is the local MOID.
- The coordinate $\zeta = \zeta(a, e, i, \Omega, \omega, f, \lambda_p)$ is related to the timing of the encounter.

The b-plane circles

It is possible to show that the locus of b-plane points for which the post-encounter orbit has a given value of a', i.e. of θ', say a'_0 and θ'_0, is a circle (VMGC00) centred on the ζ-axis, at $\zeta = D$, of radius $|R|$, with

$$\begin{aligned} D &= \frac{c \sin\theta}{\cos\theta'_0 - \cos\theta} \\ R &= \frac{c \sin\theta'_0}{\cos\theta'_0 - \cos\theta}, \end{aligned}$$

where c is a scale factor that depends on U and on the mass m of the planet in units of the solar mass:

$$c = \frac{m}{U^2}.$$

The *b*-plane circles

Such a simple property reminds us of Galileo's words:
"...[l'universo] è scritto in lingua matematica, e i caratteri son triangoli, cerchi, ed altre figure geometriche..."; it has interesting consequences:

- it is a building block of the algorithm allowing to understand the geometry of impact keyholes (VMGC03);
- it can be used to explain the asymmetric tails of energy perturbation distributions (VMGC00).

In the rest of the talk we discuss some properties of close encounters that can be deduced from this theory.

The b-plane circles

In practical applications, one has to keep in mind that:

- to each point on the b-plane of a close encounter corresponds one (and only one!) post-encounter orbit;
- for a given impact parameter b, the size of the resulting velocity deflection, and thus of the perturbation, depends critically on the ratio c/b, where $c = m/U^2$ is the impact parameter corresponding to a velocity deflection of 90°;
- a large velocity deflection does not necessarily imply a large semimajor axis perturbation.

The distribution of energy perturbations

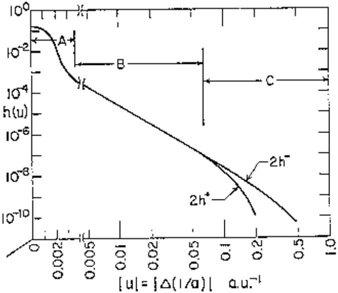

FIG. 1. The distribution $h(u)$ in energy changes u due to Jupiter is plotted vs $|u|$ for comets (otherwise random) whose Q value is 0.1 of Jupiter's orbital radius and whose inclination is 27°: The breaks in the lines indicate changeover from linear to logarithmic scales for $|u|$. The three regions A, B, and C are discussed in the text. The notation $2h^+$ indicates twice the distribution for the positive u values only, and $2h^-$ is the same for the negative u values.

The asymmetric energy perturbation distribution obtained numerically by Everhart (E69): the devil is in the (de)tails...

Cartography of the b-plane

Everhart's experiment: parabolic initial orbits, with $q/a_J = 0.1, i = 27^\circ$, i.e. $U = 1.48, \theta = 114^\circ$.

The plot shows some relevant b-plane circles.

The red circle is the collisional cross section of Jupiter, of radius $b_c = 3.3 r_p$.

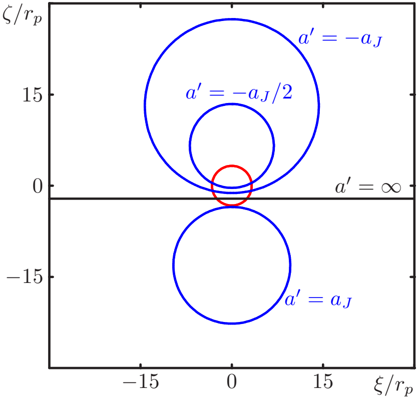

The horizontal line corresponds to parabolic post-encounter orbits.

The blue circles correspond to post-encounter orbits with $a' = a_J, a' = -a_J, a' = -a_J/2$.

Circles corresponding to different values of a' do not intersect.

Cartography of the *b*-plane

- All of Everhart's orbits have the same probability of collision with Jupiter, since Öpik's collision probability per revolution depends on U, θ, ϕ (i.e., on a, e, i) and the cross-section of the planet.
- If, instead of the planet cross-section, we consider the area of the circle corresponding to a certain post-encounter Δa, we obtain the probability of having a perturbation of size Δa or larger.

Cartography of the b-plane

Consider the circle for $a' = a_J$, within which one of Everhart's comets would be captured to an elliptical orbit of with $a' \leq a_J$.

Its area is 8.7 times larger than that the collisional cross-section of Jupiter.

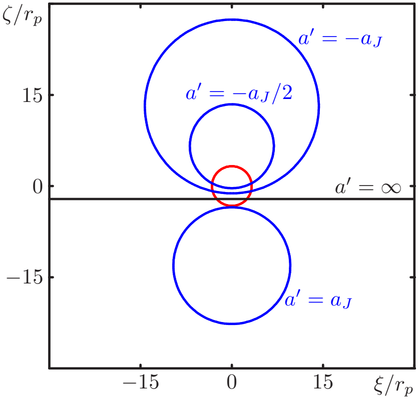

That is, for Everhart's experimental setup, capture to an orbit of period $P' \leq P_J$ is almost 9 times more frequent than collision with Jupiter.

Capture of parabolic comets to short-period orbits

Let us consider the efficiency of capture to orbits of $P \leq 200$ yr in the case of parabolic comets encountering the four outer planets.

For each planet we consider three cases:

- very high planetocentric velocity, $U = 2$, i.e., twice the heliocentric velocity of the planet;
- high planetocentric velocity, $U = 1$, i.e., the same as the heliocentric velocity of the planet;
- moderately high planetocentric velocity, $U = 0.5$, i.e., half of the heliocentric velocity of the planet.

To each of these cases correspond suitable ranges of perihelion distances and inclinations.

Comet capture by Neptune

U	b_{eff}	R	ρ	
2.0	2.4	2.6	1.2	red
1.0	4.5	19.2	18.6	blue
0.5	8.7	42.5	23.6	green

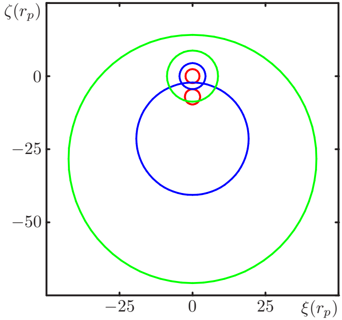

Capture to $P < 200$ yr of parabolic comets by Neptune.

Unit: planetary radius; $\rho = R^2/b_{eff}^2$.

For $U = 2$: $q = 30.1 \div 3.76$ au, $i = 110^\circ\!.7 \div 180^\circ$.

For $U = 1$: $q = 30.1 \div 15.1$ au, $i = 45^\circ\!.0 \div 0^\circ$.

For $U = 0.5$: $q = 30.1 \div 28.5$ au, $i = 13^\circ\!.5 \div 0^\circ$.

Comet capture by Uranus

U	b_{eff}	R	ρ	
2.0	1.9	4.0	4.6	red
1.0	3.3	16.9	26.3	blue
0.5	6.4	34.6	29.5	green

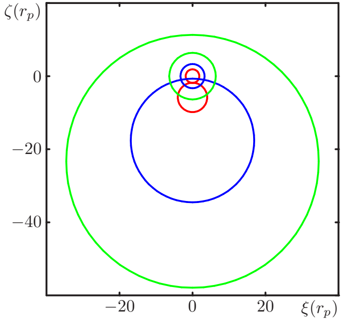

Capture to $P < 200$ yr of parabolic comets by Uranus.

Unit: planetary radius; $\rho = R^2/b_{eff}^2$.

For $U = 2$: $q = 19.2 \div 2.40$ au, $i = 110.^\circ7 \div 180^\circ$.

For $U = 1$: $q = 19.2 \div 9.6$ au, $i = 45.^\circ0 \div 0^\circ$.

For $U = 0.5$: $q = 19.2 \div 18.2$ au, $i = 13.^\circ5 \div 0^\circ$.

Comet capture by Saturn

U	b_{eff}	R	ρ	
2.0	2.1	14.4	46	red
1.0	3.9	49.7	165	blue
0.5	7.6	88.6	138	green

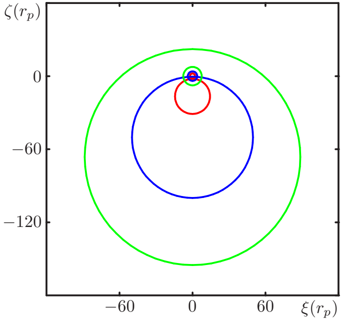

Capture to $P < 200$ yr of parabolic comets by Saturn.

Unit: planetary radius; $\rho = R^2/b_{eff}^2$.

For $U = 2$: $q = 9.54 \div 1.19$ au, $i = 110.^\circ7 \div 180^\circ$.

For $U = 1$: $q = 9.54 \div 4.77$ au, $i = 45.^\circ0 \div 0^\circ$.

For $U = 0.5$: $q = 9.54 \div 9.02$ au, $i = 13.^\circ5 \div 0^\circ$.

Comet capture by Jupiter

U	b_{eff}	R	ρ	
2.0	2.5	43.0	293	red
1.0	4.7	139	872	blue
0.5	9.3	224	583	green

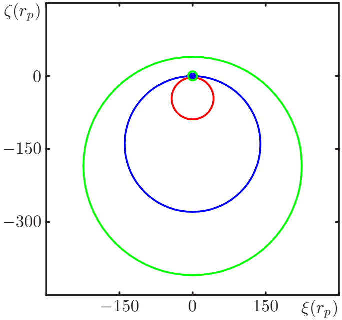

Capture to $P < 200$ yr of parabolic comets by Jupiter.

Unit: planetary radius; $\rho = R^2/b_{eff}^2$.

For $U = 2$: $q = 5.20 \div 0.65$ au, $i = 110\overset{\circ}{.}7 \div 180^\circ$.

For $U = 1$: $q = 5.20 \div 2.60$ au, $i = 45\overset{\circ}{.}0 \div 0^\circ$.

For $U = 0.5$: $q = 5.20 \div 4.92$ au, $i = 13\overset{\circ}{.}5 \div 0^\circ$.

Comet ejection by Jupiter

a	ρ	
a_J	0.26	red
$2a_J$	1.45	blue
$3a_J$	4.16	green

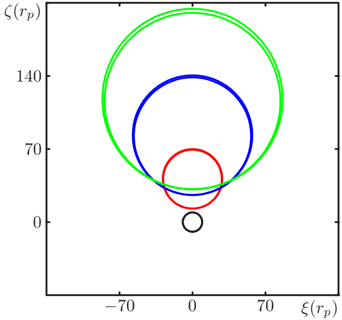

Efficiency of ejection to 1000 au $< a' < \infty$ for comets encountering Jupiter with $U = 0.5$, relative to collision with the planet.

Unit: planetary radius; $\rho = (R^2_{a'=1000} - R^2_{a'=\infty})/b^2_{eff}$.

Comet ejection by Saturn

a	ρ	
a_S	0.32	red
$2a_S$	1.76	blue
$3a_S$	5.11	green

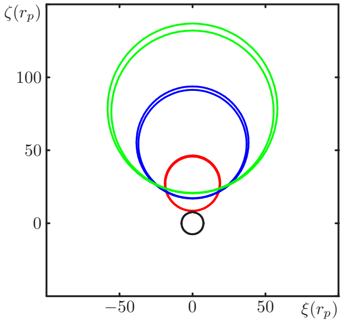

Efficiency of ejection to 1000 au $< a' < \infty$ for comets encountering Saturn with $U = 0.5$, relative to collision with the planet.

Unit: planetary radius; $\rho = (R^2_{a'=1000} - R^2_{a'=\infty})/b^2_{eff}$.

Comet ejection by Uranus

a	ρ	
a_U	0.45	red
$2a_U$	2.56	blue
$3a_U$	7.56	green

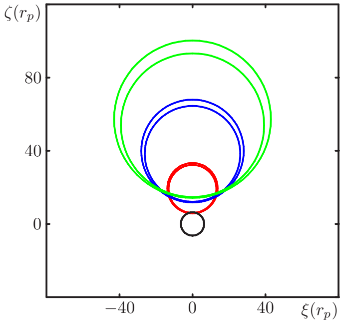

Efficiency of ejection to 1000 au $< a' < \infty$ for comets encountering Uranus with $U = 0.5$, relative to collision with the planet.

Unit: planetary radius; $\rho = (R^2_{a'=1000} - R^2_{a'=\infty})/b^2_{eff}$.

Comet ejection by Neptune

a	ρ	
a_N	1.39	red
$2a_N$	8.03	blue
$3a_N$	24.21	green

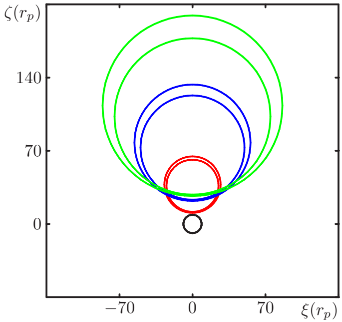

Efficiency of ejection to 1000 au $< a' < \infty$ for comets encountering Neptune with $U = 0.5$, relative to collision with the planet.

Unit: planetary radius; $\rho = (R^2_{a'=1000} - R^2_{a'=\infty})/b^2_{eff}$.

Transition prograde→retrograde

Consider a prograde orbit of given a, e, i of a comet that can encounter Jupiter; is it possible that an encounter with the latter turns the orbit into a retrograde one?

And, if yes, under what conditions?

Let us start from the expressions of U and θ as functions of a, e, i:

$$\begin{aligned} U &= \sqrt{3 - \frac{a_p}{a} - 2\sqrt{\frac{a(1-e^2)}{a_p}}\cos i} \\ \cos\theta &= \frac{1 - U^2 - \frac{a_p}{a}}{2U}. \end{aligned}$$

Transition prograde→retrograde

For $i = 90^\circ$, U becomes:

$$U = \sqrt{3 - \frac{a_p}{a}},$$

that implies:

$$\frac{a_p}{a} = 3 - U^2.$$

Substituting back in the expression for θ:

$$\cos\theta_{i=90^\circ} \quad = \quad -\frac{1}{U}.$$

This implies that transitions to retrograde orbits can take place only if $U \geq 1$, no matter what the mass of the planet is.

Transition prograde→retrograde

Thus, to obtain a transition from prograde to retrograde, we need a close encounter that changes θ into $\theta' > \theta_{i=90^\circ}$.

This is something that we know how to obtain: the *b*-plane coordinates must be within the circle of radius $|R_{i'=90^\circ}|$ centred in:

$$\begin{aligned} \xi &= 0 \\ \zeta &= D_{i'=90^\circ}, \end{aligned}$$

with $D_{i'=90^\circ}, R_{i'=90^\circ}$ given by:

$$\begin{aligned} D_{i'=90^\circ} &= \frac{c \sin\theta}{\cos\theta'_{i'=90^\circ} - \cos\theta} \\ R_{i'=90^\circ} &= \frac{c \sin\theta'_{i'=90^\circ}}{\cos\theta'_{i'=90^\circ} - \cos\theta}. \end{aligned}$$

Transition prograde→retrograde

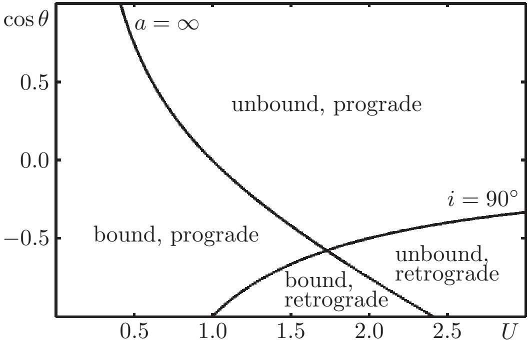

The plane U-$\cos\theta$; to each triple a, e, i corresponds a point in this plane.

Close encounters displace the orbit vertically in this plane.

Transition prograde→retrograde

For Everhart's parabolic comets ($q/a_J = 0.1$, $i = 27^\circ$), the condition $i' = 90^\circ$ implies:

$$a'_{i'=90^\circ}/a_J = 1.26.$$

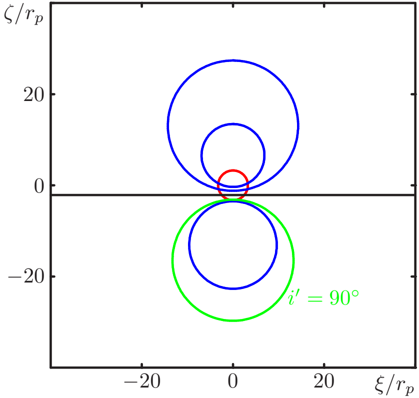

That is, all of Everhart's parabolic comets deflected in orbits of period $P \leq 1.41 P_J$ would be on retrograde post-encounter orbits.

Conclusions

The main merit of the analytical theory of close encounters is the geometric insight it provides into the problem; examples:

- the theory of resonant returns and keyholes;
- the explanation of the asymmetry of the tails of the energy perturbation distributions;
- the conditions leading to prograde-retrograde transitions and vice-versa.

Besides, its quantitative predictions can be useful in order to have a quick evaluation of the efficiency in some problems of orbital evolution dominated by planetary encounters.

References

- CVG90: Carusi A., Valsecchi G. B., Greenberg R., 1990, CeMDA 49,111
- E69: Everhart E., 1969, AJ 74, 735
- O76: Öpik E. J., 1976, Interplanetary Encounters, Elsevier
- V06: Valsecchi G. B., 2006, Lect. Notes Phys. 682, 145
- VMGC00: Valsecchi G. B., Milani A., Gronchi G. F., Chesley S. R., 2000, CeMDA 78, 83
- VMGC03: Valsecchi G. B., Milani A., Gronchi G. F., Chesley S. R., 2003, A&A 408, 1179
- VAR15: Valsecchi G. B., Alessi E. M., Rossi A., 2015, CeMDA 123, 151 (see also the Erratum, CeMDA 123, 167)